

# On the origin of fluorine in the Milky Way

A gostino R enda<sup>1?</sup>, Yeshe Fenner<sup>1?</sup>, Brad K. Gibson<sup>1?</sup>,  
A m anda I. K arakas<sup>2;3</sup>, John C. Lattanzio<sup>2</sup>, Sim on C am pbell<sup>2</sup>, A lessandro C hie <sup>1;2;4;5</sup>,  
K atia C unha<sup>6</sup>, Verne V. Sm ith<sup>7</sup>

<sup>1</sup>Centre for Astrophysics & Supercomputing, Swinburne University, Hawthorn, Victoria, 3122, Australia

<sup>2</sup>Centre for Stellar & Planetary Astrophysics, School of Mathematical Sciences, Monash University, Clayton, Victoria 3800, Australia

<sup>3</sup>Institute for Computational Astrophysics, Department of Astronomy & Physics, Saint Mary's University, Halifax, Nova Scotia B3H 3C3, Canada

<sup>4</sup>Istituto di Astrofisica Spaziale e Fisica Cosmica (CNR), Via Fosso del Cavaliere, 00133 Roma, Italia

<sup>5</sup>INAF Osservatorio Astronomico di Roma, Via Frascati 33, 00040 Monteporzio Catone, Italia

<sup>6</sup>Observatorio Nacional, Rua General Jose Cristino 77, 20921-400 Sao Cristovao, Rio de Janeiro, Brazil

<sup>7</sup>Department of Physics, University of Texas at El Paso, El Paso, TX 79968, U.S.A.

Accepted. Received; in original form

## ABSTRACT

The main astrophysical factories of fluorine (<sup>19</sup>F) are thought to be Type II supernovae, Wolf-Rayet stars, and the asymptotic giant branch (AGB) of intermediate mass stars. We present a model for the chemical evolution of fluorine in the Milky Way using a semi-analytic multi-zone chemical evolution model. For the first time, we demonstrate quantitatively the impact of fluorine nucleosynthesis in Wolf-Rayet and AGB stars. The inclusion of these latter two fluorine production sites provides a possible solution to the long-standing discrepancy between model predictions and the fluorine abundances observed in Milky Way giants. Finally, fluorine is discussed as a possible probe of the role of supernovae and intermediate mass stars in the chemical evolution history of the globular cluster  $\omega$  Centauri.

Key words: galaxies: evolution { stars: abundances { stars: evolution

## 1 INTRODUCTION

The three primary astrophysical factories for fluorine (<sup>19</sup>F) production have long been thought to be Type II Supernovae (SNe II), Wolf-Rayet (WR) stars, and asymptotic giant branch (AGB) stars (e.g. Woosley & Weaver 1995; Meynet & Aumoult 2000; Forestini et al. 1992; Mowlavi, Jorissen & Aumoult 1998, respectively). Previous attempts to model the Galactic production and evolution of <sup>19</sup>F have been restricted to explore the role of SNe II alone (e.g. Timmes, Woosley & Weaver 1995; Alves, Labay & Canal 2001).

The above problem has now been ameliorated by the release of the first detailed yield predictions for fluorine production from WR and AGB stars. We are now in a position to incorporate these yields into a Galactic chemical evolution framework, in order to assess the respective contributions of the three putative fluorine production sites. To do so, we will make use of GEtool, a semi-analytical multi-zone Galactic chemical evolution package which has been calibrated with

extant observational data for the Milky Way (Fenner & Gibson 2003; Gibson et al. 2003).

Specifically, in what follows, we compare the model fluorine distribution in the Milky Way with the abundances observed by Jorissen, Smith & Lambert (1992) in near-solar metallicity giants. Further, our model predictions are contrasted with new fluorine determinations for giants in the Large Magellanic Cloud (LMC) and  $\omega$  Centauri (Cunha et al. 2003). In addition, new results for more  $\omega$  Centauri giants from Smith et al. (2004) are included. The latter two systems are likely to have had very different star formation and chemical evolution histories from those of the Milky Way, but despite these obvious differences, a comparison against these new data can be valuable. In Section 2, we provide a cursory overview of the three traditional <sup>19</sup>F nucleosynthesis sites; the chemical evolution code in which the nucleosynthesis products from these factories have been implemented is described in Section 3. Our results are then presented and summarised in Sections 4 and 5, respectively.

? arenda,yfenner,bjgibson@astro.swin.edu.au

arXiv:astro-ph/0410580v1 25 Oct 2004

2 NUCLEOSYNTHESIS OF  $^{19}\text{F}$ 

## 2.1 Type II Supernovae

The massive star progenitors to SNe II produce fluorine primarily as the result of spallation of  $^{20}\text{Ne}$  by  $\alpha$  and neutrinos near the collapsed core (Woosley & Haxton 1988; Woosley et al. 1990). A fraction of the  $^{19}\text{F}$  thus created is destroyed by the subsequent shock but most is returned to the ambient Interstellar Medium (ISM). The fluorine yields by neutrino spallation are very sensitive to the assumed spectra of  $\alpha$  and neutrinos (Woosley et al. 2002), which could be nonthermal and deficient on their high-energy tails, lowering the equivalent temperature of the neutrinos in the supernova model (Myra & Burrows 1990). An additional source of  $^{19}\text{F}$  derives from pre-explosive CNO burning in helium shell. However, fluorine production by neutrino spallation is largely dominant, as evident by comparing the models in Woosley & Weaver (1995), the only ones to-date including neutrino process, and recent models which do not include neutrino nucleosynthesis of fluorine (Limongi & Chieffi 2003). Most recently, Heger et al. (2004) suggest that the relevant neutrino cross sections need to be revised downwards; if confirmed, the associated SNe II  $^{19}\text{F}$  yield would decrease by 50%. In light of the preliminary nature of the Heger et al. claim, we retain the conservative choice offered by the Woosley & Weaver (1995) compilation.

## 2.2 Asymptotic giant branch stars

The nucleosynthesis pathways for fluorine production within AGB stars involve both helium burning and combined hydrogen-helium burning phases (e.g. Forestini et al. 1992; Jorissen et al. 1992; Mowlaviet al. 1998) and are companions for the nucleosynthesis by slow neutron accretion (s-process) (Mowlaviet al. 1998). Provided a suitable source of protons is available, fluorine can be synthesised via  $^{14}\text{N}(\alpha, n)^{18}\text{F}(\beta^+)^{18}\text{O}(\alpha, n)^{15}\text{N}(\alpha, n)^{19}\text{F}$ . Primary sources of uncertainty in predicting fluorine nucleosynthesis in AGB stars relate to the adopted reaction rates, especially  $^{14}\text{C}(\alpha, n)^{18}\text{O}$  and  $^{19}\text{F}(\alpha, p)^{22}\text{Ne}$ , and the treatment of the nucleosynthesis occurring during the convective thermal pulses. Nucleosynthesis during the interpulse periods can also be important if protons from the envelope are partially mixed in the top layers of the He intershell (partial mixing zone), as Lugaro et al. (2004) have recently demonstrated. Nucleosynthesis in this zone may result in a significant increase in the predicted  $^{19}\text{F}$  yields. The magnitude of these systematic uncertainties for stellar models with mass  $3 M_{\odot}$  and metallicities  $Z = 0.004$ – $0.02$  are 50%, while for stellar models with mass  $M = 5 M_{\odot}$  and metallicity  $Z = 0.02$  the uncertainty is a factor of 5, due to the uncertain  $^{19}\text{F}(\alpha, p)^{22}\text{Ne}$  reaction rate. Characterising the mass- and metallicity-dependence of the partial mixing zone- $^{19}\text{F}$  relationship needs to be completed before we can assess its behaviour self-consistently within our chemical evolution model of the Milky Way. For the present study, we have adopted the yields presented in Appendix, based upon the Karakas & Lattanzio (2003, and references therein) models, which themselves do not include  $^{19}\text{F}$  nucleosynthesis via partial mixing. This choice is a conservative one, and thus should be considered as a lower limit to the production of  $^{19}\text{F}$  from AGB stars.

For stars more massive than  $4 M_{\odot}$ , the convective envelope is so deep that it penetrates into the top of the hydrogen-burning shell so that nucleosynthesis actually occurs in the envelope of the star. Such "hot-bottom-burning" acts to destroy  $^{19}\text{F}$ , and should be treated self-consistently within the AGB models considered.

## 2.3 Wolf-Rayet stars

Fluorine production in WR stars is tied to its nucleosynthesis during the helium-burning phase. At the end of this phase though, significant fluorine destruction occurs via  $^{19}\text{F}(\alpha, p)^{22}\text{Ne}$ . Any earlier synthesised  $^{19}\text{F}$  must be removed from the stellar interior in order to avoid destruction. For massive stars to be significant contributors to net fluorine production, they must experience mass loss on a timescale that allows the removal of  $^{19}\text{F}$  before its destruction. This requirement is met by WR stars.

Recently, Meynet & Aumond (2000) studied the role that such stars can play in the chemical evolution of fluorine by adopting updated reaction rates coupled with extreme mass-loss rates in non-rotating stellar models. They pointed out that WR mass-loss is strongly metallicity-dependent, and that the number of WR stars at low metallicities is very small. Their WR yields reflect such metallicity-dependence, with minimal fluorine returned to the ISM at low metallicities, but significant  $^{19}\text{F}$  returned at solar and super-solar metallicities. The WR yields are sensitive to the adopted reaction and mass-loss rates, while rotating models could favour an early entrance into the WR phase for a given mass, decrease the minimum initial mass for a star to go through a WR phase at a given metallicity, and open more nucleosynthetic channels because of the mixing induced by rotation. Therefore, after Meynet & Aumond (2000), we consider the aforementioned WR yields as lower limits.

## 3 THE MODEL

In this study we employ GETool, our semi-analytical multi-zone chemical evolution package to model a sample Milky Way-like disk galaxy (Fenner & Gibson 2003; Gibson et al. 2003). A dual-infall framework is constructed in which the first infall episode corresponds to the formation of the halo, and the second to the inside-out formation of the disk.

A Kroupa, Tout & Gilmore (1993) initial mass function (IMF) has been assumed, with lower and upper mass limits of  $0.08 M_{\odot}$  and  $120 M_{\odot}$ , respectively. Stellar yields are one of the most important features in galactic chemical evolution models, yet questions remain concerning the precise composition of stellar ejecta, due to the uncertain role played by processes including mass loss, rotation, fallback, and the location of the mass cut, which separates the remnant from the ejected material in SNe. The SNe II yields are from Woosley & Weaver (1995); the yields for stars more massive than  $60 M_{\odot}$  are assumed to be mass-independent. Such assumption is made to avoid extreme extrapolation from the most massive star in the Woosley & Weaver models ( $40 M_{\odot}$ ) to the upper end of the IMF ( $120 M_{\odot}$ ), and has negligible effect on the results, given the shape of the adopted IMF.

We have halved the iron yields shown in Woosley &

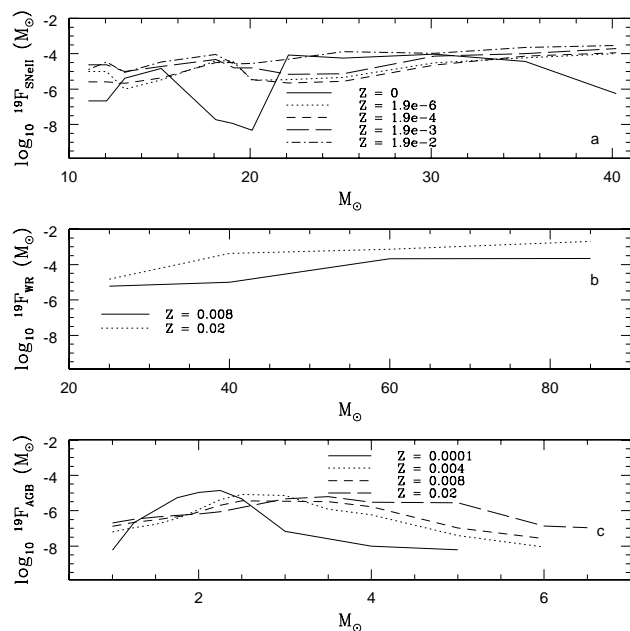


Figure 1. Fluorine yields from a) SNe II (Woosley & Weaver 1995), b) WR (Meynet & Aumond 2000), and c) AGB stars (Appendix).

Weaver (1995), as suggested by Timmes et al. (1995). The Type Ia (SNe Ia) yields of Iwamoto et al. (1999) were also employed. We adopted the metallicity-dependent yields of Renzini & Voli (1981) for single stars in the mass range  $1 - 8 M_{\odot}$ . For the purposes of this work, which focuses on fluorine, the choice of the Renzini & Voli yield set does not affect the results. Metallicity-dependent stellar lifetimes have been taken from Schaller et al. (1992).

We have constructed three Milky Way (MW) model variants that differ only in their respective treatments of  $^{19}\text{F}$  production: 1) MW a assumes that SNe II are the only source of  $^{19}\text{F}$ ; 2) MW b includes yields from both SNe II and WR stars; 3) MW c includes all three sources of fluorine – SNe II, WR, and AGB stars.

We end by noting that within our adopted dual-infall framework for the chemical evolution of the Milky Way, our model is constrained by an array of observational boundary conditions, including the present-day star and gas distributions (both in density and metallicity), abundance ratio patterns, age-metallicity relation, and G-dwarf distribution (Gibson et al. 2003). While the modification of any individual ingredient within model framework will have an impact, to some degree, upon the predicted chemical evolution, this can only eventuate at the expense of one or more of the aforementioned boundary conditions that we require our model to adhere to. Within our framework, yield uncertainties will dominate the systematic uncertainties for the predicted evolution of  $^{19}\text{F}$ .

### 3.1 Fluorine yields

We now summarise the  $^{19}\text{F}$  yields employed in our three 'Milky Way' models.

1) SNe II  $^{19}\text{F}$  yields are taken from Woosley & Weaver (1995) and assumed to be mass-independent for stellar masses in excess of  $60 M_{\odot}$ .

2) WR  $^{19}\text{F}$  yields are taken from Meynet & Aumond (2000) for stellar masses in the range  $25 - 120 M_{\odot}$ : each star within this range is assumed to evolve through the WR stage. Such simplifying assumption could overestimate the WR contribution to fluorine, even though the adopted WR yields are themselves lower limits (Section 2.3). The WR fluorine contribution has been added to the corresponding SNe II contribution (which comes from a different stage of the stellar evolution).

3) AGB  $^{19}\text{F}$  and oxygen yields in the  $1 - 6.5 M_{\odot}$  mass range have been derived from stellar models constructed with the Mount Stromlo Stellar Structure Code (Frost & Lattanzio 1996; Karakas et al. 2002), and are presented in Appendix. The post-processing nucleosynthesis models with 74 species and time-dependent diffusive convective mixing are described in detail in Frost et al. (1998) and Karakas & Lattanzio (2003).

To ensure internal consistency, we have also employed the AGB oxygen yields in lieu of those of Renzini & Voli (1981), within this mass range.

The above fluorine yields are shown in Figure 1. In Figure 2, the yields are expressed as  $[\text{F}/\text{O}]^{\dagger}$  and  $h[\text{F}/\text{O}]_{\text{IMF}}$ , the latter corresponding to the mean  $[\text{F}/\text{O}]$  yields for SNe II and AGB stars, weighted by the IMF over the SNe II and AGB mass range, respectively. We have not shown a comparable entry for the WR stars as a self-consistent treatment of the oxygen production was not included in Meynet & Aumond (2000). Here, oxygen has been used as the normalisation to make easier the comparison with the observations, especially in Centauri, though oxygen can be synthesised in various stellar sites, and its yields can be affected by different reaction rates and modeling of helium cores, semi-convection, convective boundary layers, and mass-loss (e.g. Woosley et al. 2002; Dray et al. 2003).

## 4 RESULTS

In Figure 3, the evolution of  $[\text{F}/\text{O}]$ ,  $A(\text{O})$ , the gas infall rate  $\dot{m}_{\text{infall}}$ , the star formation rate (SFR), the SNe II rate and the gas-phase global metallicity  $Z$  of the three models at the solar neighbourhood are summarised. The empirical SFR history derived by Bertelli & Nasi (2001) is shown as a thick solid line in Figure 3d, while the shaded region corresponds to the range of values suggested by Rana (1991). A conservative range of estimated SNe II rates is also shown in Figure 3e (Cappellaro, Evans & Turatto 1999).<sup>2</sup> Figure 4

<sup>1</sup> Hereafter,  $[X/Y] = \log_{10}(X/Y) - \log_{10}(X/Y)_{\odot}$  and  $A(X) = 12 + \log_{10}(n_X/n_H)$ . An accurate determination of photospheric solar abundances requires detailed modeling of the solar granulation and accounting for departures from local thermodynamic equilibrium (e.g. Allende Prieto, Lambert & Asplund 2001). We adopt the solar fluorine abundance suggested by Cunha et al. (2003), and the solar iron and oxygen abundances from Holweger (2001).

<sup>2</sup> The range of values shown in Figure 3e is derived from the sample of S0a {Sb galaxies in Cappellaro et al. (1999) – 0.42  $0.19 \text{ SNu}$ , where  $1 \text{ SNu} = 1 \text{ SN} (100 \text{ yr})^{-1} (10^{10} L^{\text{B}})^{-1}$ , assuming  $L_{\text{MW}}^{\text{B}} = 2 \cdot 10^{10} L^{\text{B}}$  and a galactic radial extent of 15 kpc.

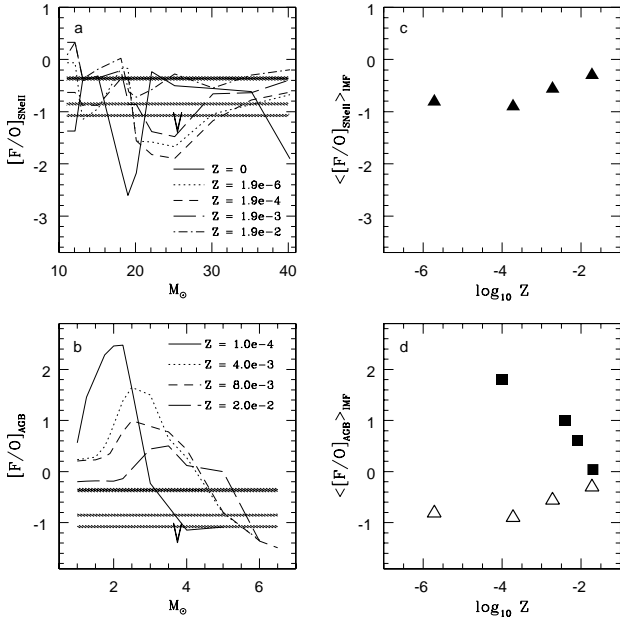


Figure 2.  $[F/O]$  and  $h[F/O]_{\text{IMF}}$  for SNe II and AGB yields (upper and lower panels, respectively). Here,  $A(^{19}\text{F}) = 4:55$  (see discussion in Cunha et al. 2003) and  $A(\text{O}) = 8:736$  (e.g. Holweger 2001). The shaded regions in Figures 2a and 2b show the observed  $[F/O]$  in  $\text{I Cen}$  giants (Cunha et al. 2003). The  $h[F/O]_{\text{IMF}}$  are weighted by the IMF over the SNe II ( $11 - 40 M_{\odot}$ ) and AGB ( $1 - 6.5 M_{\odot}$ ) mass range, respectively. In Figure 2d, both  $h[F/O]_{\text{AGB}}_{\text{IMF}}$  and  $h[F/O]_{\text{SNe II}}_{\text{IMF}}$  are shown (closed boxes and open triangles, respectively).

then shows the evolution of  $[F/O]$  versus  $A(\text{O})$  (panel a), and the evolution of  $[F/O]$  versus  $[O/Fe]$  (panel b), compared against the IMF-weighted SNe II yields (recall Figure 2).

The MW a model provides a satisfactory reproduction of the estimated star formation history and SNe II rate in the solar neighbourhood (Figures 3d and 3e). This model, whose only uorine source is SNe II, underproduces uorine with respect to the abundances measured in K and M Milky Way giants observed by Jorissen et al. (1992) and reanalysed by Cunha et al. (2003) (Fig. 4a). Fig. 4a does not show the s-process enriched AGB stars of spectral types M S, S, or C in Jorissen et al. (1992), where freshly synthesised uorine could be mixed to the stellar surface. Such inclusion of self-polluted  $^{19}\text{F}$ -rich stars could obscure any metallicity trend. The results of the MW a and MW b models show that the additional contribution from WR stars increases  $[F/O]$  by up to factor of 2 by the present-day, but it is negligible in excess of 9 Gyr ago (Figure 3c).

The addition of both WR and AGB sources within the MW c model leads to a present-day  $[F/O]$  that is 0.4 dex greater than in the MW a case. Further, and perhaps more important, AGB stars are now shown to deliver significant amounts of uorine to the ISM during the early epochs of the Milky Way's evolution. Such a result is entirely con-

Given these assumptions, the estimated SNe II rate at the solar neighbourhood is necessarily uncertain.

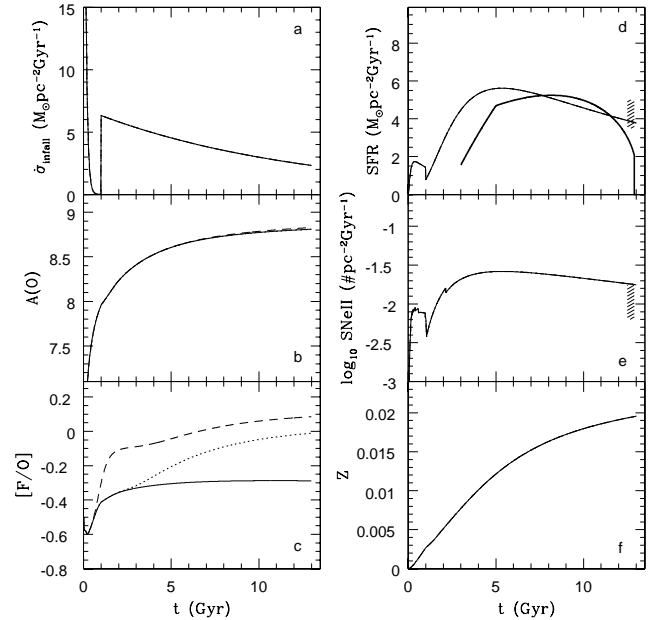


Figure 3. Predicted evolution in the solar neighbourhood of a) the gas infall rate  $\dot{\sigma}_{\text{infall}}$ , b)  $A(\text{O})$ , c)  $[F/O]$ , d) star formation rate (SFR), e) SNe II rate, and f) metallicity  $Z$  (MW a, solid line; MW b, dotted; MW c, short-dashed). The SFR history at the solar neighbourhood obtained by Bertelli & Nasi (2001) is also shown as a thick solid line in panel d', while the shaded region shows the range of values suggested by Rana (1991). A range of values corresponding to the estimated SNe II rate is shown in panel e' (Cappellaro et al. 1999).

sistent (and expected) given the metallicity-dependence of the AGB yields; said yields possess  $[F/O]$  ratios which are greater at lower metallicities (recall Figure 2). We can conclude that it is only the addition of both the WR and AGB contributions which allow for a significant improvement in the comparison between galactic models incorporating uorine evolution and the observational data.

## 5 DISCUSSION

We have studied the Galactic chemical evolution of uorine, for the first time using new grids of stellar models which provide self-consistent predictions of uorine nucleosynthesis for stars in both the WR and AGB phases of stellar evolution. We have shown that the WR contribution is significant at solar and super-solar metallicities because of the adopted metallicity-dependent mass-loss prescription employed in the stellar models. In contrast, the contribution of AGB stars to uorine production peaks during the early epochs of the Galaxy's evolution (again due to the metallicity-dependent behaviour of the AGB models). In combination, the addition of the WR and AGB yields leads to a significant improvement in the galactic chemical evolution models when compared against observations.

The comparison between our MW models and the uorine abundances in LMC and  $\text{I Cen}$  giants (Cunha et al. 2003) is not straightforward, as the latter two have star for-

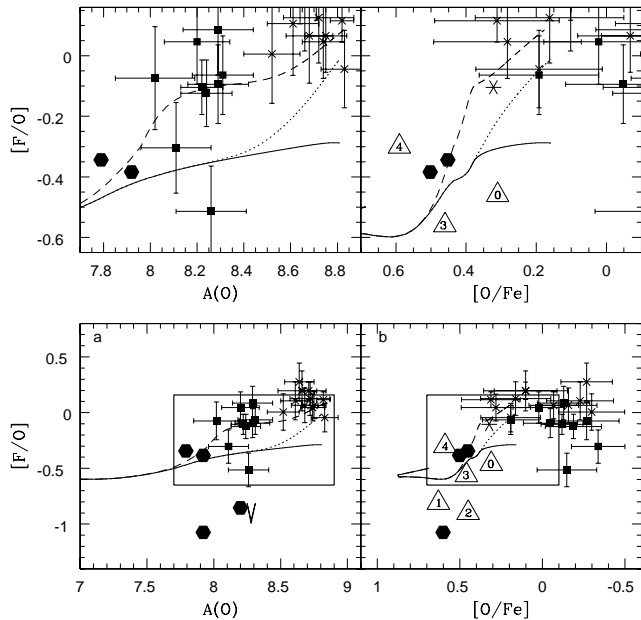


Figure 4. (a):  $[F/O]$  as a function of  $A(O)$  for the MW models (MW a, solid line; MW b, dotted; MW c, short-dashed). Also shown are the values observed in Milky Way, LMC, and ICen giants (crosses, boxes and hexagons, respectively). (b):  $[F/O]$  as a function of  $[O/Fe]$ , compared with the IMF-weighted  $[O/Fe]$  yields for SNe II (open triangles). Within the open triangles, 1' corresponds to  $Z = 0$ ; 1'', to  $Z = 1.9 \times 10^{-6}$ ; 2', to  $Z = 1.9 \times 10^{-4}$ ; 3', to  $Z = 1.9 \times 10^{-3}$ ; 4', to  $Z = 1.9 \times 10^{-2}$ . The upper panels represent enlargements of the framed regions delineated in the corresponding bottom panels.

mation (and therefore chemical evolution) histories different from that of the MW. However, it is interesting to speculate on the possible origin of fluorine in ICen, given the unique nature of this "globular cluster" (e.g. Smith 2003). Specifically, ICen is the most massive Galactic cluster, and unlike most globulars, possesses a significant spread in metallicity ( $\sim 1.5$  dex) amongst its stellar population. It has been suggested that ICen is actually the remnant core of a tidally-disrupted dwarf galaxy (Bekki & Freeman 2003). Such a scenario could naturally drive radial gas inflows to the dwarf nucleus, potentially triggering starbursts.

Interestingly, SNe II ejecta are characterised by low  $h[F/O]_{\text{IMF}}$  (Figure 2c) and high  $h[D/Fe]_{\text{IMF}}$  (Figure 4b), whereas AGB ejecta have higher  $h[F/O]_{\text{IMF}}$  (Figure 2d). The observed ICen giants have primarily low  $[F/O]$  (Figures 2a & 2b, 4a & 4b) and high  $[D/Fe]$  (Figure 4b) values, consistent with a picture in which their interiors have been polluted by the ejecta of an earlier generation of SNe II, but not from a comparable generation of AGB. Given that the observed oxygen abundance in such ICen giants is similar to that seen in comparable LMC and MW giants (Figure 4a), this would suggest that the chemical enrichment of ICen proceeded on a short timescale (to avoid pollution from the lower mass progenitors to the AGB stars) and in an inhomogeneous manner (given the significant scatter in observed fluorine abundances), as discussed previously by Cunha et al. (2003). Should the (downward) revised neutrino cross

sections alluded to in Section 2.1 be confirmed (Heger et al. 2004), the concurrent factor of  $\sim 2$  reduction in SNe II  $^{19}\text{F}$  production would improve the agreement of the model with the observed  $F/O$  ratio in ICen giants. This would consequently strengthen our conclusions which already support a picture whereby these giants have been polluted by earlier generations of SNe II ejecta.

#### ACKNOWLEDGMENTS

We acknowledge the financial support of the Australian Research Council through its Discovery Project and Linkage International schemes, and the Victorian Partnership for Advanced Computing through its Expertise Grant program. We thank Maria Lugaro for discussion and help, and the referee, Marcel A. Mould, for his comments. We also acknowledge the efforts of toothpaste manufacturers around the world in highlighting the importance of fluorine production throughout the Universe.

#### REFERENCES

- Alibés A., Labay J., Canal R., 2001, *A & A*, 370, 1103  
 Allende Prieto C., Lambert D. L., Asplund M., 2001, *ApJ*, 556, L63  
 Bekki K., Freeman K. C., 2003, *MNRAS*, 346, L11  
 Bertelli G., Nasi E., 2001, *AJ*, 121, 1013  
 Cappellaro E., Evans R., Turatto M., 1999, *A & A*, 351, 459  
 Cunha K., Smith V. V., Lambert D. L., Hinkle K. H., 2003, *AJ*, 126, 1305  
 Dray L. M., Tout C. A., Karakas A. I., Lattanzio J. C., 2003, *MNRAS*, 338, 973  
 Fenner Y., Gibson B. K., 2003, *PASA*, 20, 189  
 Forestini M., Goriely S., Jorissen A., A. Mould M., 1992, *A & A*, 261, 157  
 Frost C. A., Lattanzio J. C., 1996, *ApJ*, 473, 383  
 Frost C. A., Cannon R. C., Lattanzio J. C., Wood P. R., Forestini M., 1998, *A & A*, 332, L17  
 Gibson B. K., Fenner Y., Renda A., Kawata D., Lee H.-c., 2003, *PASA*, 20, 401  
 Heger A., Kolbe E., Haxton W. C., Langanke K., Martínez-Pinedo G., Woosley S. E., 2004, preprint (astro-ph/0307546)  
 Holweber H., 2001, in Wimmer-Schweingruber R. F., ed., *AI P Conf. Proc. 598, "Solar and Galactic Composition"*. Am. Inst. Phys., New York, p. 23  
 Iglesias C. A., Rogers F. J., 1996, *ApJ*, 464, 943  
 Iwamoto K., Brachwitz F., Nomoto K., Kishimoto N., Umehata H., Hix W. R., Thielemann F.-K., 1999, *ApJS*, 125, 439  
 Jorissen A., Smith V. V., Lambert D. L., 1992, *A & A*, 261, 164  
 Karakas A. I., Lattanzio J. C., Pols O. R., 2002, *PASA*, 19, 515  
 Karakas A. I., Lattanzio J. C., 2003, *PASA*, 20, 279  
 Kroupa P., Tout C. A., Gilmore G., 1993, *MNRAS*, 262, 545  
 Linongi M., Chieffi A., 2003, *ApJ*, 592, 404  
 Lugaro M., Ugalde C., Karakas A. I., Gorres J., Wiescher M., Lattanzio J. C., Cannon R. C., 2004, *ApJ* in press (astro-ph/0407551)

- Meynet G., Aumond M., 2000, *A & A*, 355, 176  
 Mowlavi N., Jorissen A., Aumond M., 1998, *A & A*, 334, 153  
 Myra E.S., Burrows A., 1990, *ApJ*, 364, 222  
 Rana N.C., 1991, *ARA & A*, 29, 129  
 Renzini A., Voli M., 1981, *A & A*, 94, 175  
 Russell S.C., Dopita M.A., 1992, *ApJ*, 384, 508  
 Schaller G., Schaerer D., Meynet G., Maeder A., 1992, *A & AS*, 96, 269  
 Smith V.V., 2003, in McWilliam A., Rauch M. eds, *Carnegie Observatories Astrophysics Series, Vol. 4: Origin and Evolution of the Elements*, (Pasadena: Carnegie Observatories, <http://www.ociw.edu/ociw/symposia/series/symposium4/proceedings.html>)  
 Smith V.V., Cunha K., Hinkle K.H., Blum R.D., 2004, submitted  
 Tinnes F.X., Woosley S.E., Weaver T.A., 1995, *ApJS*, 98, 617  
 Vassiliadis E., Wood P.R., 1993, *ApJ*, 413, 641  
 Woosley S.E., Haxton W.C., 1988, *Nature*, 334, 45  
 Woosley S.E., Hartmann D.H., Hoeman R.D., Haxton W.C., 1990, *ApJ*, 356, 272  
 Woosley S.E., Weaver T.A., 1995, *ApJS*, 101, 181  
 Woosley S.E., Heger A., Weaver T.A., 2002, *Rev. Mod. Phys.*, 74, 1015

zone was ignored in the models presented here. Primary sources of uncertainty in predicting uranium nucleosynthesis in AGB stars relate to the adopted reaction rates, especially  $^{14}\text{C}(\alpha, n)^{18}\text{O}$  and  $^{19}\text{F}(\alpha, p)^{22}\text{Ne}$ , and the treatment of the nucleosynthesis occurring during the convective thermal pulses and the interpulse periods (Lugaro et al. 2004; see also Section 2.2).

This paper has been typeset from a  $\text{T}_\text{E}\text{X}/\text{L}_\text{A}\text{T}_\text{E}\text{X}$  file prepared by the author.

#### APPENDIX A: ASYMPTOTIC GIANT BRANCH $^{19}\text{F}$ AND $^{16,17,18}\text{O}$ YIELDS

The yields employed here have been derived via the following:

$$Y_{^{19}\text{F}; \text{O}}(Z) = \frac{Y_{\text{net}^{19}\text{F}; \text{O}}}{X_{^{19}\text{F}; \text{O}}(Z) - [m_{\text{rem}}(Z)]} \quad (\text{A } 1)$$

Here,  $Y_{^{19}\text{F}; \text{O}}(Z)$  is the overall yield,  $X_{^{19}\text{F}; \text{O}}(Z)$  is the initial mass fraction of the element within a star of mass  $m_{\text{star}}$  and metallicity  $Z$ ,  $[m_{\text{rem}}(Z)]$  is the total mass ejected during the stellar lifetime, and  $Y_{\text{net}^{19}\text{F}; \text{O}}$  is the net yield. We calculate  $X_{^{16}\text{O}}$  and  $Y_{\text{net}^{16}\text{O}}$  as, respectively:

$$X_{^{16}\text{O}} = X_{^{16}\text{O}} + X_{^{17}\text{O}} + X_{^{18}\text{O}}; \quad (\text{A } 2)$$

$$Y_{\text{net}^{16}\text{O}} = Y_{\text{net}^{16}\text{O}} + Y_{\text{net}^{17}\text{O}} + Y_{\text{net}^{18}\text{O}}; \quad (\text{A } 3)$$

The yields are the result of full evolutionary calculations using the Mount Stromlo Stellar Structure Code (e.g. Karakas & Lattanzio 2003). We use the standard Reimers mass-loss formula on the first giant branch and the Vassiliadis & Wood (1993) formula during the AGB evolution. Opacities are from OPAL (Iglesias & Rogers 1996). The models with  $Z = 0.02$  and  $0.0001$  used scaled solar abundances, whereas those for  $Z = 0.004$  and  $0.008$  are appropriate to the Small and Large Magellanic Clouds, respectively, and are taken from Russell & Dopita (1992). Numerical problems during the third dredge-up are handled in the way described in Frost & Lattanzio (1996). A mixing length of 1.75 pressure scale-heights has been used. A main uncertainty in the predicted yields for uranium is the occurrence and dimension of the partial mixing zone. Note that this partial mixing

Table A.1. AGB  $^{19}\text{F}$  and  $^{16,17,18}\text{O}$  yields ( $M_{\odot}$ ).

Z		$X_{i_{19}\text{F}}$	$X_{i_{16}\text{O}}$	$X_{i_{17}\text{O}}$	$X_{i_{18}\text{O}}$
0.0001		2.31800e-09	4.44786e-05	1.93800e-08	1.08000e-07
$m_{\odot}$	$m_{\odot}$ rem	$Y_{\text{net } 19\text{F}_{\text{AGB}}}$	$Y_{\text{net } 16\text{O}_{\text{AGB}}}$	$Y_{\text{net } 17\text{O}_{\text{AGB}}}$	$Y_{\text{net } 18\text{O}_{\text{AGB}}}$
1.0	0.65	0.51379E-08	0.52869E-05	0.38546E-07	-0.59145E-08
1.25	0.65	0.21202E-06	0.69519E-04	0.72848E-07	-0.14220E-07
1.75	0.67	0.54275E-05	0.31623E-03	0.60806E-06	0.21305E-07
2.0	0.70	0.10527E-04	0.41221E-03	0.78911E-06	0.66983E-07
2.25	0.72	0.13578E-04	0.51952E-03	0.41433E-06	0.99055E-07
2.5	0.737	0.45574E-05	0.13068E-02	0.74846E-06	-0.17541E-07
3.0	0.820	0.62016E-07	0.13776E-02	0.20197E-05	-0.23173E-06
4.0	0.868	0.27367E-08	0.16630E-02	0.36273E-05	-0.33571E-06
5.0	0.924	-0.34142E-08	0.76699E-03	0.19749E-05	-0.41578E-06
Z		$X_{i_{19}\text{F}}$	$X_{i_{16}\text{O}}$	$X_{i_{17}\text{O}}$	$X_{i_{18}\text{O}}$
0.004		1.69218E-07	1.28324E-03	1.41477E-06	7.88419E-06
$m_{\odot}$	$m_{\odot}$ rem	$Y_{\text{net } 19\text{F}_{\text{AGB}}}$	$Y_{\text{net } 16\text{O}_{\text{AGB}}}$	$Y_{\text{net } 17\text{O}_{\text{AGB}}}$	$Y_{\text{net } 18\text{O}_{\text{AGB}}}$
1.0	0.63	0.94462E-09	-0.29158E-05	0.22240E-06	-0.25334E-06
1.25	0.64	0.62277E-08	-0.20669E-05	0.49241E-06	-0.89206E-06
1.5	0.646	0.22912E-07	0.19546E-04	0.15093E-05	-0.15635E-05
1.75	0.65	0.17284E-06	0.75738E-04	0.44914E-05	-0.25162E-05
1.9	0.65	0.49608E-06	0.95973E-04	0.75796E-05	-0.32065E-05
2.25	0.66	0.38720E-05	0.14749E-03	0.11186E-04	-0.43546E-05
2.5	0.68	0.80892E-05	0.93431E-04	0.98989E-05	-0.54950E-05
3.0	0.73	0.68954E-05	0.16497E-04	0.10204E-04	-0.69500E-05
3.5	0.82	0.76727E-06	0.62994E-04	0.43600E-05	-0.19736E-04
4.0	0.86	0.55804E-07	0.68820E-05	0.17349E-05	-0.24560E-04
5.0	0.91	-0.65262E-06	-0.19071E-02	0.20350E-05	-0.32029E-04
6.0	0.97	-0.84234E-06	-0.39748E-02	0.10162E-05	-0.39405E-04
Z		$X_{i_{19}\text{F}}$	$X_{i_{16}\text{O}}$	$X_{i_{17}\text{O}}$	$X_{i_{18}\text{O}}$
0.008		3.25423E-07	2.64027E-03	2.72075E-06	1.51621E-05
$m_{\odot}$	$m_{\odot}$ rem	$Y_{\text{net } 19\text{F}_{\text{AGB}}}$	$Y_{\text{net } 16\text{O}_{\text{AGB}}}$	$Y_{\text{net } 17\text{O}_{\text{AGB}}}$	$Y_{\text{net } 18\text{O}_{\text{AGB}}}$
1.0	0.5998	0.23717E-08	-0.26083E-05	0.28610E-06	-0.39665E-06
1.25	0.61	0.11401E-07	-0.40814E-05	0.65704E-06	-0.15151E-05
1.5	0.63	0.20168E-07	-0.45432E-05	0.19727E-05	-0.28219E-05
1.75	0.64	0.90125E-07	0.22020E-04	0.60267E-05	-0.45889E-05
1.9	0.64	0.18749E-06	0.38094E-04	0.95185E-05	-0.53377E-05
2.25	0.65	0.14941E-05	0.85696E-05	0.16553E-04	-0.74497E-05
2.5	0.67	0.30357E-05	-0.12452E-03	0.14976E-04	-0.90888E-05
3.5	0.77	0.22972E-05	-0.37752E-03	0.16132E-04	-0.14133E-04
4.0	0.84	0.66878E-06	-0.30252E-03	0.14747E-04	-0.23226E-04
5.0	0.89	-0.12324E-05	-0.24193E-02	0.68396E-05	-0.61869E-04
6.0	0.95	-0.16173E-05	-0.57759E-02	0.80141E-05	-0.75982E-04
Z		$X_{i_{19}\text{F}}$	$X_{i_{16}\text{O}}$	$X_{i_{17}\text{O}}$	$X_{i_{18}\text{O}}$
0.02		4.63728E-07	9.60266E-03	3.87707E-06	2.16506E-05
$m_{\odot}$	$m_{\odot}$ rem	$Y_{\text{net } 19\text{F}_{\text{AGB}}}$	$Y_{\text{net } 16\text{O}_{\text{AGB}}}$	$Y_{\text{net } 17\text{O}_{\text{AGB}}}$	$Y_{\text{net } 18\text{O}_{\text{AGB}}}$
1.0	0.57309	0.36025E-08	-0.61933E-06	0.34219E-06	-0.41416E-06
1.25	0.578	0.15858E-07	-0.22254E-05	0.97603E-06	-0.18066E-05
1.5	0.60	0.25014E-07	-0.32904E-05	0.31910E-05	-0.33975E-05
1.75	0.63	0.29957E-07	-0.54827E-05	0.90611E-05	-0.52622E-05
1.9	0.636	0.28199E-07	-0.10482E-04	0.14418E-04	-0.60505E-05
2.0	0.64	0.27049E-07	-0.17893E-04	0.19332E-04	-0.66536E-05
2.25	0.65	0.12064E-06	-0.20851E-03	0.44894E-04	-0.81507E-05
3.0	0.682	0.34981E-05	-0.11882E-02	0.51877E-04	-0.13306E-04
3.5	0.716	0.49320E-05	-0.17086E-02	0.57427E-04	-0.17219E-04
4.0	0.791	0.14844E-05	-0.16979E-02	0.55128E-04	-0.19531E-04
5.0	0.878	0.86376E-06	-0.39096E-02	0.46522E-04	-0.70118E-04
6.0	0.929	-0.22147E-05	-0.83059E-02	0.78725E-04	-0.10882E-03
6.5	0.964	-0.24583E-05	-0.97865E-02	0.98794E-04	-0.11879E-03